

Investigation of desolvation process in lanthanide dinicotinates

R. Łyszczek · M. Iwan

Received: 1 June 2010 / Accepted: 13 October 2010 / Published online: 3 November 2010
© Akadémiai Kiadó, Budapest, Hungary 2010

Abstract The desolvation process in lanthanide pyridine-3,5-dicarboxylates of the formulae $[\text{Tb}_2\text{pdc}_3(\text{dmf})_2]\cdot\text{dmf}$ (**1**), $[\text{Ho}_2\text{pdc}_3(\text{dmf})_2]\cdot\text{dmf}$ (**2**), $[\text{Erdc}_3(\text{dmf})_2]\cdot\text{dmf}$ (**3**), and $[\text{Yb}_2\text{pdc}_3(\text{dmf})_2]\cdot\text{dmf}$ (**4**) where $\text{pdc}=\text{C}_5\text{H}_3\text{N}(\text{COO})_2^{2-}$, $\text{dmf}=\text{N,N}'\text{-dimethylformamide}$ has been investigated by means of the TG–DSC, TG–FTIR, IR and XRD methods. Heating of the complexes in the range 30–260 °C lead to evolution of weakly bonded dmf molecules included in the channels as well those directly bonded with lanthanide atoms. The kinetic analysis revealed a multistep desolvation pattern.

Keywords Lanthanide dinicotinates · Desolvation · Thermal analysis · Analysis of products · Kinetic analysis

Introduction

There has been considerable interest in coordination polymers known as metal–organic frameworks (MOFs) due to their promising applications such as the molecular recognition and separation from the gaseous and liquid mixtures, storage of gases, catalysis and drug delivery [1–3]. Coordination polymers can also be designed as multifunctional materials with the additional physical properties like magnetism, luminescence and optoelectronics [4, 5]. The construction of architectures of metal–organic frameworks consists of the assembly of highly coordinated metal centres/clusters with multifunctional organic linkers. The structural properties of the components determine the

topology and porosity of the target materials. The resulting complexes are in the form of 1-, 2- or 3-D structures, with or without channels, filled by solvent molecules or co-crystallizing organic molecules incorporated during synthesis [6, 7]. These molecules can be regarded as templates exterminating the pore sizes and shapes. Usually, these guest molecules can be removed upon heating of ‘as-made’ sample under reduced pressure and the obtained framework retains the initial structure, resulting in a porous material [8–10]. On the other hand, the removal of the included in cavities molecules can lead to structure collapsing that results in formation of amorphous phases. For some complexes this process is reversible and the amorphous-to-crystal transformation can take place [11].

Taking into consideration behaviour of metal–organic frameworks during activation, coordination polymers can be divided into three categories: (1) the first generation of coordination polymers is of the microporous structures which show irreversible framework collapse after removal of the guest molecules. (2) The second generation of metal–organic frameworks remains porous and crystalline without any guest molecules in the pores. (3) The third generation of coordination polymers is of dynamic and flexible structures which respond to external stimuli (like guest molecules, light and electric field) in changing their structures) to change shape and size of channels. The transformation in the second and third generations is named ‘crystal-to-crystal’ [12, 13].

The solvent molecules used in the synthesis of coordination polymers, not only occupy free space in the channels, but also may take part in the coordination process being directly bonded with the metal centre [14–19]. $\text{N,N}'\text{-dimethylformamide}$ (dmf) is a very popular solvent applied in the synthesis of lanthanide coordination polymers. Polarity of dmf molecules is crucial in the growth process

R. Łyszczek (✉) · M. Iwan
Department of General and Coordination Chemistry, Faculty of Chemistry, University of Maria Curie-Skłodowska, Sq. M.C. Skłodowskiej 2, 20-031 Lublin, Poland
e-mail: renata.lyszczek@poczta.umcs.lublin.pl

of crystals. Dmf dissolves well not only most of the organic ligands but also inorganic lanthanide species that facilitates formation of crystalline forms of complexes.

The aim of this study was to investigate the desolvation process in the complexes of selected heavy lanthanides(III) with the pyridine-3,5-dicarboxylate ligand. These metal-organic frameworks were obtained by solvothermal method from the *N,N'*-dmf solution. The complexes were previously investigated in detail by means of elemental analysis, infrared spectroscopy, X-ray powder and single crystal diffractions as well as different methods of thermal analysis [20].

The investigated complexes form the three-dimensional expanded polymeric network with one-dimensional channels occupied by solvent molecules. The coordination environment of central atoms consists of carboxylate oxygen atoms from pyridine-3,5-dicarboxylate moieties. In addition, the coordination sphere of metal centres is completed by oxygen atom from dmf molecules. The complexes reported herein possess 1-D channels along the crystallographic *a* axis occupied by disordered dmf molecules [17, 18]. The complexes decompose in two well-separated weight loss steps. The first one is connected with the removal of solvent molecules included in the channels as well as coordinated with metal centres. The second stage is attributed to the decomposition and burning (air) of the desolvated form of complexes.

Transformation of coordination polymers into their porous form is preceded by the activation process, connected with removal of solvent molecules from the channels as well as rearrangement of their crystal structures. Activation of lanthanide complexes with pyridine-3,5-dicarboxylic and dmf molecules occurs after the loss of free and coordinated solvent molecules that results in formation of crystalline stable Ln_2pdc_3 frameworks. These materials are porous and can effectively adsorb nitrogen as well as benzene molecules [18].

In addition, this article deals with the determination of kinetic parameters of desolvation step connected with release of coordinated dmf molecules determined using the AKTS Thermokinetics Software program [21].

Experimental

The studied compounds were synthesized via solvothermal method in 150 mL teflon-lined autoclaves. The 1.5 mmol of pyridine-3,5-dicarboxylic acid (dinicotinic acid) (250 mg) with lanthanide(III) chloride hydrates (obtained by dissolving of 0.5 mmol of lanthanide oxide in hydrochloric acid) were dissolved in 10 mL of *N,N'*-dmf. The autoclaves were heated in oven for 5 days at 140 °C and then cooled to room temperature for 24 h. Needle-shaped crystals were separated from a clear solution.

The X-ray powder diffractions of the studied complexes were recorded on a HZG 4 diffractometer using Ni filtered CuK_α radiations. Measurements were taken over the range of $2\theta = 5\text{--}70^\circ$.

Thermal analysis of prepared complexes was carried out by the TG–DSC method using SETSYS 16/18 analyser (Setaram). The samples (about 5–7 mg) were heated in a ceramic crucible up to 850 °C at a heating rate of 10 °C min^{-1} in dynamic air atmosphere ($v = 0.75 \text{ dm}^3 \text{ h}^{-1}$). For kinetic measurements, the heating rates: 5, 2.5 and 1.25 °C min^{-1} were applied.

The TG–FTIR coupled measurements have been carried out using a Netzsch TG apparatus coupled with a Bruker FTIR IFS66 spectrophotometer. The samples of about 30 mg were heated up to 950 °C at a heating rate of 10 °C min^{-1} in flowing argon atmosphere.

The samples of as-made complexes of about 0.1 g were heated at 100 and 250 °C during 2 h in drying apparatus Binder.

Results and discussion

The investigations of desolvation process of heavy lanthanides [Tb(III), Ho(III), Er(III) and Yb(III)] complexes with pyridine-3,5-dicarboxylic acid of the formulae: $[\text{Tb}_2\text{pdc}_3(\text{dmf})_2]\cdot\text{dmf}$, $[\text{Ho}_2\text{pdc}_3(\text{dmf})_2]\cdot\text{dmf}$, $[\text{Er}_2\text{pdc}_3(\text{dmf})_2]\cdot\text{dmf}$, and $[\text{Yb}_2\text{pdc}_3(\text{dmf})_2]\cdot\text{dmf}$ (where $\text{pdc}=\text{C}_5\text{H}_3\text{N}(\text{COO})_2^-$, dmf-*N,N'*-dimethylformamide) molecules have been carried out. The complexes in question have been obtained as unstable needle monocystals. When transparent crystals are exposed to the air, they partially lose solvent molecules that can be observed by making crystals dull.

Thermal analysis

The thermal stability of the investigated complexes has been studied in the air as well as in the argon atmosphere using the TG–DSC and TG–FTIR methods. It could be mentioned that during heating of the complexes in the temperature range 30–450 °C, they behave in the same manner under both the conditions. Thermal properties as well as kinetic investigations of the studied complexes were performed in air. As can be seen in Fig. 1, the complexes are stable up to about 30 °C and then start to decompose. Under air condition, on the TG curves in the temperature range 30–260 °C weight losses of 22.42, 20.42, 20.64, 21.17 and 21.00% for complexes 1, 2, 3 and 4, respectively, were found. This stage matches well the removal of solvent molecules from the crystal structures (calculated mass losses are 20.93, 20.97, 20.89 and 20.67% for 1, 2, 3 and 4, respectively). Mass loss observed in the lower temperature range 30°–100 °C, is connected with release of weakly bonded dmf molecules included in the

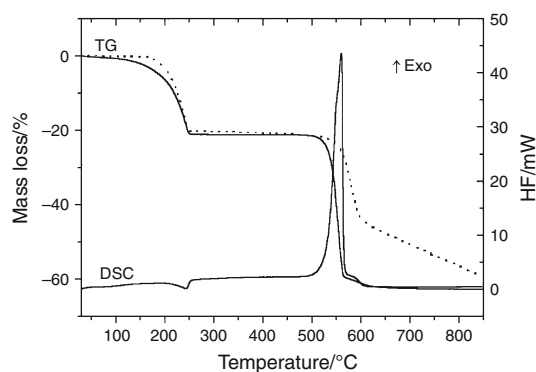


Fig. 1 TG–DSC curves of $[\text{Ho}_2\text{pdc}_3(\text{dmf})_2]\cdot\text{dmf}$ recorded in air (solid line) and argon (dashed line)

channels of the crystal frameworks. Further heating of the complexes resulted in dissociation of bonds between carbonyl oxygen from dmf molecules and lanthanide atoms. The dmf molecules release from the coordination environments of lanthanide ions is accompanied by distinct endothermic effects on the DSC curves (111–60 kJ/mol) at temperatures 257, 252, 253 and 252 °C (peak top) for compounds 1, 2, 3 and 4, respectively. Further heating cause decomposition of desolvated forms of complexes which is accompanied with burning of organic ligand (air atmosphere). As the solid residue of thermal decomposition, the corresponding oxides: Tb_4O_7 , Ho_2O_3 , Er_2O_3 and Yb_2O_3 (in air) or mixture of oxides and carbon (in argon atmosphere) are formed [20].

The TG–FTIR technique was applied as the method providing more information about the reaction sequences and the relevant products of decomposition especially in the temperature range of desolvation. Since the pathways of degradation under both conditions up to 450 °C are the same, the results obtained by means of the TG–FTIR method were applied to the data obtained from the thermogravimetric analysis in air condition.

As can be seen from the FTIR spectrum of gaseous products of the desolvation process (Fig. 2) recorded at 175 °C, there are bands derived from gaseous N,N' -dimethylformamide molecules. The bands at 2939 and

2849 cm^{-1} were assigned to the asymmetric and symmetric stretching vibrations of the CH bond from the CH_3 groups. Methyl groups of dmf molecules also give characteristic bands derived from asymmetric and symmetric deformation vibrations at 1482 and 1382 cm^{-1} , respectively. The band located at 1724 cm^{-1} can be attributed to the stretching vibrations of the carbonyl CO group. The band at 1493 cm^{-1} was assigned to stretching vibrations of the CN bond [22]. The highest intensity of these bands is observed at about 220 °C. Removal of dmf molecules distributed within channels and those coordinated resulted in the formation of Ln_2pdc_3 compounds relatively stable in the temperature range 260–460 °C that is confirmed by the absence of any bands on the FTIR spectra. Next, collapse and decomposition of the frameworks take place. Decomposition of the desolvated form of the complexes is connected with evolution of carbon dioxide molecules giving characteristic doublet bands at 2359, 2343 cm^{-1} and those in the range 750–600 cm^{-1} ascribed to the valence and deformation vibrations, respectively (530 °C) [23]. At little higher temperature, further gaseous products of thermal decomposition were recorded. The bands at 3075, 3017 and 1217, 1152 cm^{-1} were assigned to the stretching and deformation vibrations of C–C and C–N groups from the free pyridine ring. The double-band with the maxima at 2177 and 2113 cm^{-1} was derived from carbon monoxide. Moreover, some unidentified hydrocarbons were released due to the presence of bands at 3071, 1605, 1484 and 1448 cm^{-1} [24].

The most interesting stage during thermal decomposition of the studied complexes is release of solvent molecules from the crystal structures of the complexes. Heating the complexes up to 250 °C in air atmosphere under atmospheric pressure leads to cracking of crystals. They are still crystalline but still intransparent that excludes them in further single crystal X-ray measurements. The infrared spectra of the obtained compounds confirm release of dmf molecules from the crystal structures. The IR spectra of desolvated complexes do not show characteristic bands derived from the dmf molecules compared with as-made complexes. There are not observed stretching vibrations of

Fig. 2 Stacked plot of FTIR spectra of the evolved gases for $[\text{Ho}_2\text{pdc}_3(\text{dmf})_2]\cdot\text{dmf}$

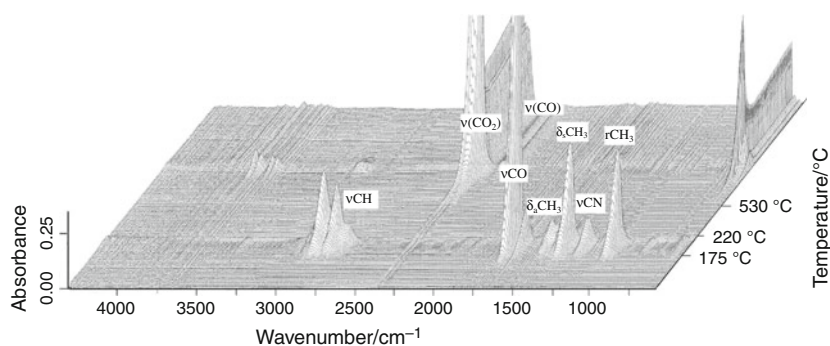


Fig. 3 IR spectra of complex *a* $[\text{Ho}_2\text{pdc}_3(\text{dmf})_2]\cdot\text{dmf}$; *b* after heating at 250 °C

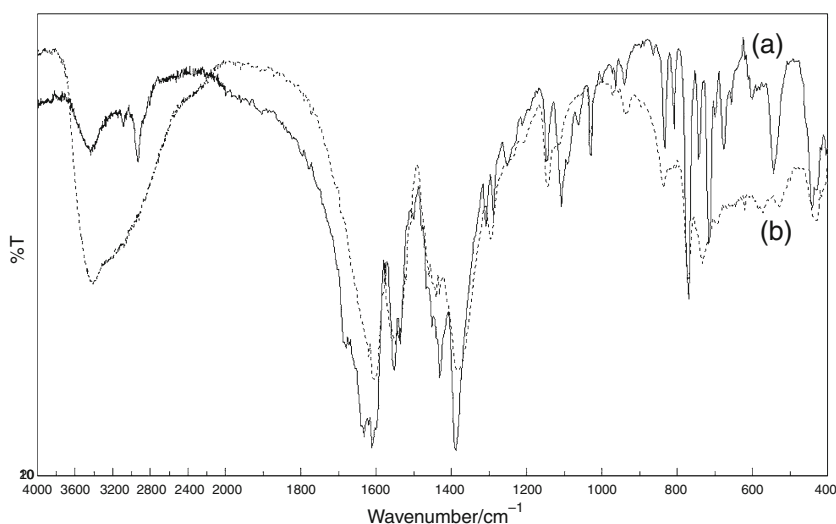


Table 1 Most characteristic bands (cm^{-1}) in the IR spectra of **1**, **2**, **3** and **4** complexes and their desolvated forms

	νCH_3	νCO (dmf)	$\nu_{\text{as}} \text{COO}$	$\nu_{\text{sym}} \text{COO}$
$[\text{Tb}_2\text{pdc}_3(\text{dmf})_2]\cdot\text{dmf}$ (1)	3062, 2940	1668	1632, 1600	1384
Tb_2pdc_3	–	–	1604	1380
$[\text{Ho}_2\text{pdc}_3(\text{dmf})_2]\cdot\text{dmf}$ (2)	3092, 2928	1680, 1651	1632, 1612	1388
Ho_2pdc_3	–	–	1608	1384
$[\text{Er}_2\text{pdc}_3(\text{dmf})_2]\cdot\text{dmf}$ (3)	3092, 2928	1688, 1656	1640, 1612	1388
Er_2pdc_3	–	–	1604	1384
$[\text{Yb}_2\text{pdc}_3(\text{dmf})_2]\cdot\text{dmf}$ (4)	3092, 2928	1688, 1656	1640, 1610	1380
Yb_2pdc_3	–	–	1608	1388

CH_3 groups in the wavenumber range 3000–2900 cm^{-1} as well as stretching vibrations from carbonyl group in the range 1690–1650 cm^{-1} derived from the dmf molecules (Fig. 3). Moreover, as can be seen from Table 1, the characteristic bands derived from stretching asymmetric and symmetric vibrations of carboxylate groups in the infrared spectra of desolvated complexes are shifted compared with those in as-made complexes. In addition, the bands of the asymmetric stretching vibrations of COO groups observed in IR spectra of heated complexes are not split as it takes place for as-made complexes.

The powder X-ray diffractions were performed for the as-synthesized samples, and those heated at 100 and 250 °C. The XRD patterns for the samples heated at 100 °C are similar to those of as-made samples, which indicates that release of guest molecules from the channels does not lead to collapse of the crystal structure (Fig. 4).

The X-ray powder diffraction patterns of the samples heated at 250 °C revealed that they remain crystalline.

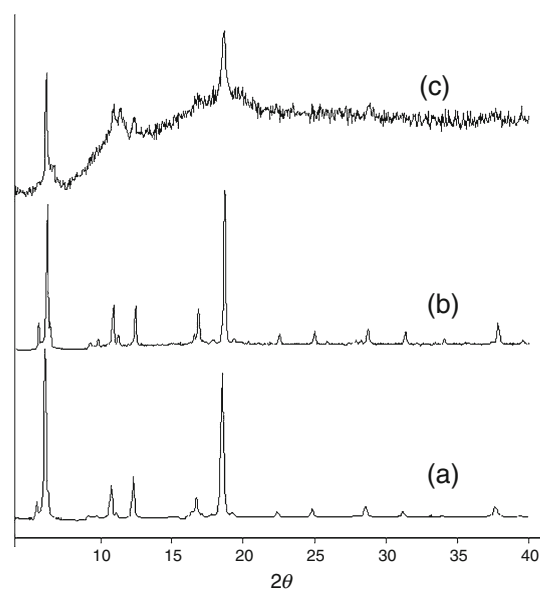


Fig. 4 XRD patterns of *a* original solid $[\text{Ho}_2\text{pdc}_3(\text{dmf})_2]\cdot\text{dmf}$; *b* after heating at 100 °C for 2 h; *c* after heating at 250 °C for 2 h

Comparison of the XRD results of as-made complexes with the heated samples leads to the conclusion that departure of the guest molecules and the coordinated dmf molecules does not cause the collapse of the crystal structures. This result indicates formation of stable frameworks composed of lanthanide atoms and dinicotinate ligands during heating. As can be seen in Fig. 4, the most intense reflexes in the heated sample are observed at slightly higher values of 2θ (6.26, 10.95, 11.45, 12.35 and 18.70) compared with those of as-made complexes (6.05, 10.35, 10.75, 12.10 and 18.25). This data may point to some transformation in their crystal structures that is indicative for crystal-to-crystal transformation. Since, the dmf molecules were bonded with lanthanide ions, their removal from the coordination

environment of metals resulted in rearrangement of coordination mode of carboxylate groups.

The kinetic investigations

The TG data collected during non-isothermal decomposition of the sample with the heating rates of 1.25, 2.5 and 5 °C min⁻¹ in the dynamic air atmosphere were used for determination of the kinetic parameters of the dmf removal reaction. The data were analysed by the AKTS Thermokinetics Software using the model-free method, called the Friedman method [21, 25–28]. The calculations were made within the temperature range of 100–260 °C. It corresponds to the loss of coordinated dmf molecules. The first step of thermal decomposition of lanthanide dinicotinates (30–100 °C), i.e., the stage of release of the weakly bonded solvent molecules, is not appropriate for kinetic accounts.

The TG signals after correction of the baseline were used to estimate the reaction progress. Figure 5 presents the reaction rate as a function of temperature for lanthanide dinicotinate desolvation. Comparison of the experimental (symbols) and the simulated courses of the reaction (lines) indicated a very good fit when the kinetic analysis was used. The rate maximum falls in the range of 210–230 °C. It coincides with the highest intensity of dmf bands in the FTIR spectra of gaseous products of thermal decomposition. Figure 6 illustrates the results of the Friedman analysis, and Fig. 7 shows the activation energies and pre-exponential factors for the desolvation of the compounds investigated. The changes in the values of E and A during the course of the reaction indicate a complex multistep desolvation pattern [29]. They account well for the two consecutive stages of dmf molecule release from the compounds investigated.

Fig. 5 Reaction rate as a function of temperature for terbium **a**, holmium **b**, erbium **c** and ytterbium **d** dinicotinate desolvation. Experimental data are represented as *symbols* and the calculated signals as *solid lines*. Notation on curves: the heating rate in °C min⁻¹

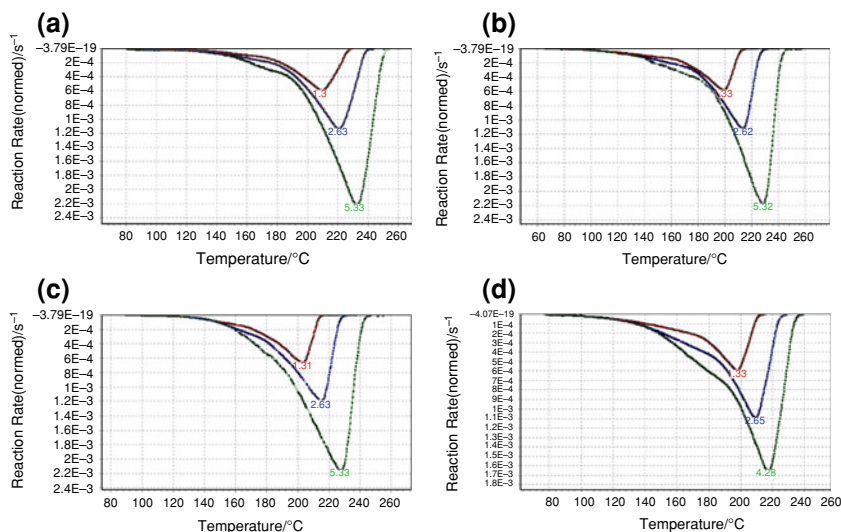


Fig. 6 Friedman analysis for the desolvation of terbium **a**, holmium **b**, erbium **c** and ytterbium **d** dinicotinates

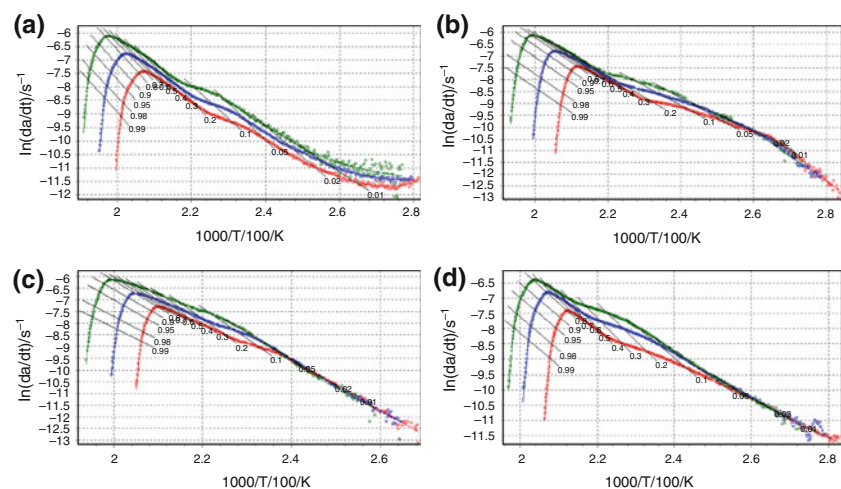
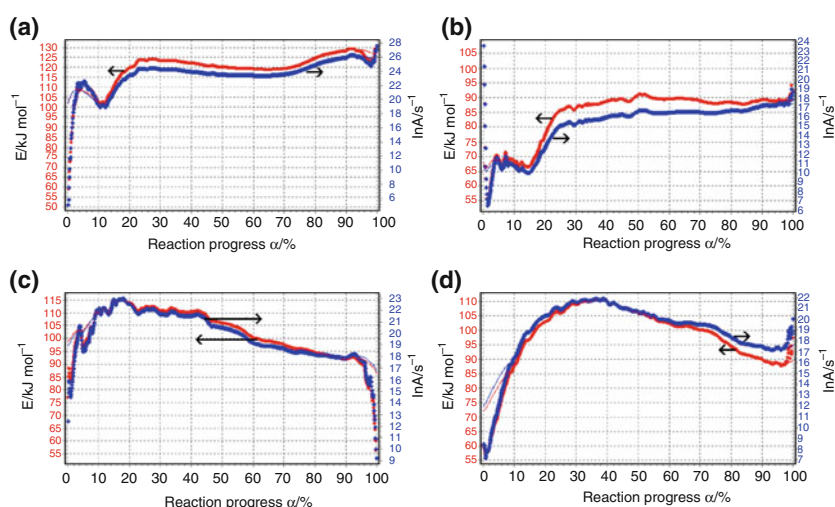


Fig. 7 Activation energy, E and pre-exponential factor, A values as a function of the reaction progress for the desolvation of terbium **a**, holmium **b**, erbium **c** and ytterbium **d** dinicotinates



Conclusions

The desolvation process in the studied complexes was investigated by means of the thermal analysis TG–DSC. It is connected with the release of the dmf molecules from the channels as well as those bonded with metal centres as confirmed by the TG–FTIR analysis. The solid products of desolvation of the formula $\text{Ln}_2\text{pdc}_3(\text{dmf})_2$ retain their crystalline forms as follows from the XRD patterns. The calculated values of the kinetic parameters refer to the reaction of removal of dmf molecules from the inner coordination sphere of lanthanide atoms. The activation energies obtained are characteristic of the multistep process.

References

1. Czaja AU, Trukhan N, Müller U. Industrial applications of metal-organic frameworks. *Chem Soc Rev.* 2009;38:1284–93.
2. Ferey G. Some suggested perspectives for multifunctional hybrid porous solids. *Dalton Trans.* 2009;23:4400–15.
3. Kesanli B, Lin W. Chiral porous coordination networks: rational design and applications in enantioselective processes. *Coord Chem Rev.* 2003;246:305–26.
4. Lu W-G, Jiang L, Feng X-L, Lu T-B. Three-dimensional lanthanide anionic metal-organic frameworks with tunable luminescent properties induced by cation exchange. *Inorg Chem.* 2009;48:6997–9.
5. Flores M, Caldiño U, Córdoba G, Arroyo R. Luminescent enhancement of Eu^{3+} -doped poly(acrylic acid) using 1,10-phenanthroline as antenna ligand. *Optical Mat.* 2004;27:635–9.
6. Janiak C. Engineering coordination polymers towards applications. *Dalton Trans.* 2003;14:2781–804.
7. Robin AY, Fromm KM. Coordination polymer networks with O- and N-donors: what they are, why and how they are made. *Coord Chem Rev.* 2006;250:2127–57.
8. Senkovska I, Hoffman F, Fröba M, Getzschmann J, Böhlmann W, Kaskel S. New highly porous aluminium based metal-organic frameworks: $\text{Al}(\text{OH})(\text{ndc})$ ($\text{ndc} = 2$, 6-naphthalene dicarboxylate) and $\text{Al}(\text{OH})(\text{bpdc})$ ($\text{bpdc} = 4$, 4'-biphenyl dicarboxylate). *Micropor Mesopor Mater.* 2009;122:93–8.
9. Haitao X, Zhihua L. Microporous rare-earth coordination polymers constructed by 1, 4-cyclohexanedicarboxylate. *Micropor Mesopor Mater.* 2008;118:522–6.
10. Dietzel PDC, Panella B, Hirscher M, Bloom R, Fjellvåg H. Hydrogen adsorption in a nickel based coordination polymer with open metal sites in the cylindrical cavities of the desolvated framework. *Chem Commun.* 2006;9:959–61.
11. Choi HJ, Lee TS, Suh MP. Self-assembly of a molecular floral lace with one-dimensional channels and inclusion of glucose. *Angew Chem Int Ed.* 1999;38:1405–8.
12. Uemuru K, Matsuda R, Kitagawa S. Flexible microporous coordination polymers. *J Solid State Chem.* 2005;178:2420–9.
13. Kitagawa S, Uemura K. Dynamic porous properties of coordination polymers inspired by hydrogen bonds. *Chem Soc Rev.* 2005;34:109–19.
14. Wang XF, Zhang Y-B, Huang H, Zhang J-P, Chen X-M. Microwave-assisted solvothermal synthesis of a dynamic porous metal-carboxylate framework. *Crystal Growth Des.* 2008;8:4559–63.
15. Roques N, Maspoch D, Imaz I, Dacu A, Sutter J-P, Rovira C, Veciana J. A three dimensional lanthanide-organic radical open framework. *Chem Commun.* 2008;27:3160–62.
16. Guo X, Zhu G, Sun F, Li Z, Zhao X, Li X, Wang H, Qiu S. Synthesis, structure, and luminescent properties of microporous lanthanide metal-organic frameworks with inorganic rod-shaped building units. *Inorg Chem.* 2006;45:2581–7.
17. Chen B, Wang L, Xiao Y, Fronczek FR, Xue M, Cui Y, Qian G. A luminescent metal-organic framework with lewis basic pyridyl sites for the sensing of metal ions. *Angew Chem.* 2009;121:508–11.
18. Jia J, Lin X, Blake AJ, Champness NR, Hubberstey P, Shao L, Walker G, Wilson C, Schröder M. Triggered ligand release coupled to framework rearrangement: generating crystalline porous coordination materials. *Inorg Chem.* 2006;45:8838–40.
19. Wang G, Song T, Fan Y, Xu J, Wang M, Wang L, Zhang L, Wang L. A porous lanthanide metal-organic framework with luminescent property, nitrogen gas adsorption and high thermal stability. *Inorg Chem Commun.* 2010;13:95–7.
20. Łyszczek R. Synthesis, structure, thermal and luminescent behaviors of lanthanide—pyridine-3,5-dicarboxylate frameworks series. *Termochim Acta.* 2010. doi:10.1016/j.tca.2010.06.010.
21. <http://www.akts.com>.
22. McCann K, Laane J. Raman and infrared spectra and theoretical calculations of dipicolinic acid, dinicotinic acid, and their dianions. *J Mol Struct.* 2008;890:346–58.

23. Zapata B, Balmaseda J, Fregoso-Israel E, Torres-Garcia E. Thermo-kinetics study of orange peel in air. *J Therm Anal Cal.* 2009;98:309–15.
24. Souza BS, Moreira Ana Paula D, Teixeira Ana Maria RF. TG–FTIR coupling to monitor the pyrolysis products from agricultural residues. *J Therm Anal Cal.* 2009;97:637–42.
25. Roduit B, Borgeat Ch, Berger B, Folly P, Andres H, Schädeli U, Vogelsanger B. Up-scaling of DSC data of high energetic materials. *J Therm Anal Cal.* 2006;85:195–202.
26. Roduit B. Prediction of the progress of solid-state reactions under different temperature modes. *Thermochim Acta.* 2002;388:377–87.
27. López FA, Ramirez MC, Pons JA, López-Delgado A, Alguacil FJ. Kinetic study of the thermal decomposition of low-grade nickeliferous laterite ores. *J Therm Anal Cal.* 2008;94:517–22.
28. Rudjak I, Kaljuvee T, Trikkel A, Mikli V. Thermal behaviour of ammonium nitrate prills coated with limestone and dolomite powder. *J Therm Anal Cal.* 2010;99:749–54.
29. Zhan D, Cong Ch, Diakite K, Tao Y, Zhang K. Kinetics of thermal decomposition of nickel oxalate dihydrate in air. *Thermochim Acta.* 2005;430:101–5.